

**Current Distribution Models for the Earth's Main Magnetic Field: A Discrete
Inverse Theory Approach**

Terence V. Sowards
Sandia Research Center
21 Perdiz Canyon Road
Placitas, N.M. 87043

tsewards@yahoo.com

Abstract

Current source models for the Earth's main geomagnetic field are calculated employing conventional discrete inverse theory methods. Source structures are spherical surfaces placed at the surface of the Earth's core, and at the surface of the Earth. The data set consists of measurements taken by the MAGSAT satellite in 1979. The resulting current distributions are discussed in relation to dipole and current loop models.

1. Introduction

The Earth's main magnetic field is generated by an electric current distribution, presumably located within the Earth or near the Earth's surface. At the present time, it is generally thought that the current distribution lies in the core, and that it is generated by a magnetohydrodynamic dynamo. Determining the structure of this current distribution is an essential problem in geomagnetism. However, while it is possible to calculate the magnetic field for any given current distribution using the Biot-Savart law, the opposite problem - determining the current structure from measurements of the magnetic field - is less straightforward, and requires an inverse theory approach. To date, source models that predict the main geomagnetic field have been limited to monopoles, dipoles and current loops (Peddie, 1979; Zidarov and Petrova, 1979; Alldredge, 1980; Fraser-Smith, 1987; O'Brien and Parker, 1994). Dipole and current loop source models are reviewed in Langel (1987). The usual procedure is to select the number of dipoles or current loops and vary their position and strength until the best possible configuration is obtained.

This work addresses the problem of determining models of current distributions (rather than loops) that accurately predict the main geomagnetic field obtained from the MAGSAT satellite, employing conventional discrete inverse theory methods (Tarantola, 1987; Menke, 1989).

2. Inverse Problem Formulation

In the forward problem of geomagnetism, which is governed by the Biot-Savart law, one obtains the vector magnetic induction $\mathbf{B}(\mathbf{r})$ at the field point \mathbf{r} as a function of the vector current density $\mathbf{J}(\mathbf{r}_1)$ at the source point \mathbf{r}_1 :

$$\mathbf{B}(\mathbf{r}) = \frac{\mu_0}{4\pi} \int_{v_1} \frac{1}{R^3} \mathbf{J}(\mathbf{r}_1) \times (\mathbf{r} - \mathbf{r}_1) dv_1 \quad (1)$$

in which $R = |\mathbf{r} - \mathbf{r}_1|$. In Cartesian components,

$$\mathbf{J}(\mathbf{r}_1) = \mathbf{a}_x J_x + \mathbf{a}_y J_y + \mathbf{a}_z J_z \quad (2)$$

$$R = [(x - x_1)^2 + (y - y_1)^2 + (z - z_1)^2]^{1/2} \quad (3)$$

From these expressions, the Cartesian coordinates of $\mathbf{B}(\mathbf{r})$ may be evaluated:

$$\begin{aligned}
B_x &= -\frac{\mu_0}{4\pi} \int_{v_1} \frac{1}{R^3} [J_{z_1}(y - y_1) - J_{y_1}(z - z_1)] dv_1 \\
B_y &= -\frac{\mu_0}{4\pi} \int_{v_1} \frac{1}{R^3} [J_{x_1}(z - z_1) - J_{z_1}(x - x_1)] dv_1 \\
B_z &= -\frac{\mu_0}{4\pi} \int_{v_1} \frac{1}{R^3} [J_{y_1}(x - x_1) - J_{x_1}(y - y_1)] dv_1
\end{aligned} \tag{4}$$

Since the geomagnetic inverse problem has spherical symmetry, it is convenient to transform to spherical coordinates. This procedure results in the following expressions for the field components:

$$\begin{aligned}
B_r &= -\frac{\mu_0}{4\pi} \int_{v_1} [k_r J_{r_1} + l_r J_{\theta_1} + m_r J_{\phi_1}] dv_1 \\
B_\theta &= -\frac{\mu_0}{4\pi} \int_{v_1} [k_\theta J_{r_1} + l_\theta J_{\theta_1} + m_\theta J_{\phi_1}] dv_1 \\
B_\phi &= -\frac{\mu_0}{4\pi} \int_{v_1} [k_\phi J_{r_1} + l_\phi J_{\theta_1} + m_\phi J_{\phi_1}] dv_1
\end{aligned} \tag{5}$$

in which

$$\begin{aligned}
k_r &= 0 \\
l_r &= -r \sin(\theta) \sin(\phi - \phi_1) / R^3 \\
m_r &= r_1 [\sin \theta \cos \theta_1 \cos(\phi - \phi_1) - \cos \theta \sin \theta_1] / R^3
\end{aligned} \tag{6}$$

$$\begin{aligned}
k_\theta &= r \sin \theta_1 \sin(\phi - \phi_1) / R^3 \\
l_\theta &= [r \cos \theta_1 - r_1 \cos \theta] \sin(\phi - \phi_1) / R^3 \\
m_\theta &= [r_1 (\sin \theta \sin \theta_1 + \cos \theta \cos \theta_1 \cos(\phi - \phi_1)) - r \cos(\phi - \phi_1)] / R^3
\end{aligned} \tag{7}$$

$$\begin{aligned}
k_\phi &= r [\cos \theta \sin \theta_1 \cos(\phi - \phi_1) - \sin \theta \cos \theta_1] / R^3 \\
l_\phi &= [r (\sin \theta \sin \theta_1 + \cos \theta \cos \theta_1 \cos(\phi - \phi_1)) - r_1 \cos(\phi - \phi_1)] / R^3 \\
m_\phi &= [r \cos \theta \sin(\phi - \phi_1) - r_1 \cos \theta_1 \sin(\phi - \phi_1)] / R^3
\end{aligned} \tag{8}$$

The fact that k_r is zero means that a radial source current produces no magnetic field. Hence the radial field B_r can be modeled by only two current components, J_{θ_1} and J_{ϕ_1} . Because of this characteristic, the data set chosen is restricted to values of the radial field. The data set then has the form $B_r^{(i)}$, $i = 1, 2, 3, \dots, N_d$, with N_d being the number of data. The geometry of the source area needs to be specified, and, for the sake of simplicity, a spherical surface is chosen. The radius of this surface is then chosen such that the current is restricted to (a) the surface of the core, and (b) the surface of the Earth, for the purpose of comparison. In order to obtain a continuous model current distribution in the source area while using a discrete set of parameters, the components of the spherical surface current source are expanded in the truncated spherical harmonic series:

$$J_{\theta_1} = \sum_{m=0}^{m_{\max}} \sum_{k=0}^m P_m^k(\cos \theta_1) [A_m^k \cos(k \phi_1) + B_m^k \sin(k \phi_1)]$$

$$J_{\phi_1} = \sum_{m=0}^{m_{\max}} \sum_{k=0}^m P_m^k(\cos \theta_1) [C_m^k \cos(k \phi_1) + D_m^k \sin(k \phi_1)]$$
(9)

in which the terms $P_m^k(\cos \theta_1)$ are the associated Legendre polynomials. Substitution of these expressions into equations (5) yields

$$B_r(r, \theta, \phi) = -\frac{\mu_0}{4\pi} \sum_{m=0}^{m_{\max}} \sum_{k=0}^m [I_1 A_m^k + I_2 B_m^k + I_3 C_m^k + I_4 D_m^k]$$
(10)

in which

$$I_1 = \int_{s_1} l_r P_m^k(\cos \theta_1) \cos(k \phi_1) ds_1$$

$$I_2 = \int_{s_1} l_r P_m^k(\cos \theta_1) \sin(k \phi_1) ds_1$$

$$I_3 = \int_{s_1} m_r P_m^k(\cos \theta_1) \cos(k \phi_1) ds_1$$

$$I_4 = \int_{s_1} m_r P_m^k(\cos \theta_1) \sin(k \phi_1) ds_1$$
(11)

If the data set consists of N_d values of $B_r(r, \theta, \phi)$ distributed over the surface of the spherical current source, then for each magnetic datum there is a corresponding equation (10). The functions l_r and m_r contain the variables r , θ and ϕ , as well as the distance R between the source and field (data) points.

The summations over m and k in equation (10) can be replaced by a single summation over another index, say j . That is to say,

$$\sum_m \sum_k \rightarrow \sum_j \quad (12)$$

The coefficients $A_m^k, B_m^k, C_m^k, D_m^k$ can then be arranged as sets of numbers A_j, B_j, C_j, D_j , which are then organized into a single column vector \mathbf{m} :

$$\mathbf{m} = [A_1, B_1, C_1, D_1, A_2, B_2, C_2, D_2, \dots, D_{j_{\max/4}}]^T \quad (13)$$

The entire inverse problem can now be expressed in a single matrix equation. Calling the data $d_i = B_r(r_i, \theta_i, \phi_i)$, this equation is written as

$$\mathbf{d} = \mathbf{G} \mathbf{m} \quad (14)$$

where the matrix elements G_{ij} of \mathbf{G} are given by

$$\begin{aligned} G_{ij}^{(A)} &= -\frac{\mu_0}{4\pi} \int_{s_1} l_r^{(i)} P_m^k(\cos \theta_1) \cos(k\phi_1) ds_1 \\ G_{ij}^{(B)} &= -\frac{\mu_0}{4\pi} \int_{s_1} l_r^{(i)} P_m^k(\cos \theta_1) \sin(k\phi_1) ds_1 \\ G_{ij}^{(C)} &= -\frac{\mu_0}{4\pi} \int_{s_1} m_r^{(i)} P_m^k(\cos \theta_1) \cos(k\phi_1) ds_1 \\ G_{ij}^{(D)} &= -\frac{\mu_0}{4\pi} \int_{s_1} m_r^{(i)} P_m^k(\cos \theta_1) \sin(k\phi_1) ds_1 \end{aligned} \quad (15)$$

Equation (14) represents the standard linear inverse problem of discrete inverse theory (Menke, 1989). Although a solution \mathbf{m} of the problem yields a finite set of numbers $m_1, m_2, m_3, \dots, m_{N_m}$, because the model is based on spherical harmonic expansions the end result is a continuous current model on a spherical surface.

3. Inversion

When the problem posed by equation (14) is overdetermined, meaning that there are more data points than model parameters, the usual way to invert it is to employ either the least squares or singular value decomposition (SVD) method. Here the latter method is chosen, although it was found that least squares solutions were very similar to those

obtained by the SVD method. In the SVD paradigm, the kernel matrix \mathbf{G} is decomposed as follows:

$$\mathbf{G} = \mathbf{U} \mathbf{S} \mathbf{V}^T \quad (16)$$

in which \mathbf{U} is $N_d \times N_d$ and \mathbf{V} is $N_m \times N_m$. The matrix \mathbf{S} is $N_d \times N_m$ and diagonal, its elements are the singular values of \mathbf{G} . These are arranged in decreasing order, and truncated at the p^{th} term in order to stabilize the inversion when the matrix \mathbf{G} is ill-conditioned (Menke, 1989; Hansen, 1990). The solution is then

$$\mathbf{m}_{est} = \mathbf{V}_p \mathbf{S}_p^{-1} \mathbf{U}_p^T \mathbf{d} \quad (17)$$

where \mathbf{V}_p and \mathbf{U}_p consist of the first p columns of \mathbf{V} and \mathbf{U} respectively, \mathbf{S}_p^{-1} is the inverse of the truncated (square) singular value matrix \mathbf{S}_p , and \mathbf{m}_{est} is the vector of estimated model parameters. The numerical computation of the singular value decomposition was executed using the LINPACK software (Dongarra et al., 1979).

4. Data Set

The data employed in this study are 808 globally distributed MAGSAT measurements of the vertical (B_r) field taken on Nov. 4 - 7, 1979. These were magnetically quiet days, with low values for the parameter K_p . They were chosen from a reduced data set of 15,837 points provided by R.A. Langel of Goddard Space Flight Center, from which anomalous points had been removed. The reduction from 15,837 to 808 points was accomplished by specifying an even spacing of approximately 2250 Km between adjacent (consecutive, in terms of spacecraft motion) points. The coverage over the poles is considerably denser than over equatorial latitudes. The r.s.s. error for the B_r values is approximately 6 nT (Langel and Estes, 1985). Details of the MAGSAT mission, including the spacecraft's trajectory, are described in Langel (1982) and Langel et al. (1982).

5. Results

As mentioned above, the two source current distributions chosen were the surface of the core, and the surface of the Earth itself. The truncation level m_{max} for the spherical harmonic expansion of the components of the current was chosen to be 12.

5.1 Core Surface Model

The chosen singular value cutoff value for this model ($p = 99$) coincides with a small gap in the singular value spectrum. The total prediction error for this value of p , which is given by the formula $E = (\mathbf{d} - \mathbf{G} \mathbf{m}_{est})^T (\mathbf{d} - \mathbf{G} \mathbf{m}_{est})$ is about $3.23 \times 10^5 \text{ nT}^2$, so the

r.m.s. prediction error per datum is $\langle e \rangle = [E / N_d]^{1/2} = 20$ nT. Contours of the current densities J_{ϕ_1} as a function of θ_1 and ϕ_1 are shown in Fig. 1. As may be seen in the chart, J_{ϕ_1} is characterized by a fairly broad band of negative current at North-equatorial latitudes, a narrower band of positive current at northern latitudes, and a mixed negative/positive band at Southern latitudes. The contour map for J_{θ_1} (Fig. 2) is more complex, with patches of positive and negative current distributed over the surface of the core (Fig. 2).

5.2 Earth Surface Model

The singular value cutoff value of 193 was chosen because all singular values beyond this number are essentially noise. With this value, the total prediction error E is only 2.02×10^4 nT², corresponding to a small r.m.s. error of $\langle e \rangle = 5.0$ nT. Contours of the current distribution J_{ϕ_1} as a function of θ_1 and ϕ_1 is shown in Fig. 1. In comparison with the corresponding distribution for the core surface model, the Earth surface J_{ϕ_1} distribution is quite simple. It is everywhere negative, and is concentrated at mid-latitudes, with a strong maximum over Southeast Asia. The chart displays a noticeable similarity to the contour map of the X component of the 1980 GSFC(12/83) model at the Earth's surface (Langel, 1987), which was also computed from MAGSAT data. The only significant difference is that the latter map has a region in the Antarctic where the sign of the field is reversed, whereas the J_{ϕ_1} map is negative everywhere. The J_{θ_1} contours are more complex (Fig. 2), and resemble those for the Y component of the 1980 GSFC(12/83) model (Langel, 1987), although this resemblance is not as strong as that for the J_{ϕ_1} current. Overall, the absolute magnitude of the J_{θ_1} current is significantly lower than the magnitude of J_{ϕ_1} (Fig. 2).

6. Discussion

Modeling the geomagnetic field with spherical surface current distributions placed within the Earth's core and on its surface yields solutions that much more realistic than those provided by dipole and current loop models. The method applied here is not limited to models in which the source structure is 2-dimensional and spherical. Extension to spherical solid spheres is easily accomplished by expanding the current in the radial dimension using spherical Bessel functions. More generally, any continuous source structure that has spherical, cylindrical, or rectangular symmetry can be modeled by series expansions, and after truncation yields a finite set of parameters that effectively describes the continuous model. Then, if the data consists of a finite set of measurements, the inverse problem can be expressed in the form of equation (14), and a solution obtained via the SVD method as in equation (17), or by some other method. This is highly desirable, as the discrete inverse theory method is considerably simpler than its continuous counterpart (Menke, 1989).

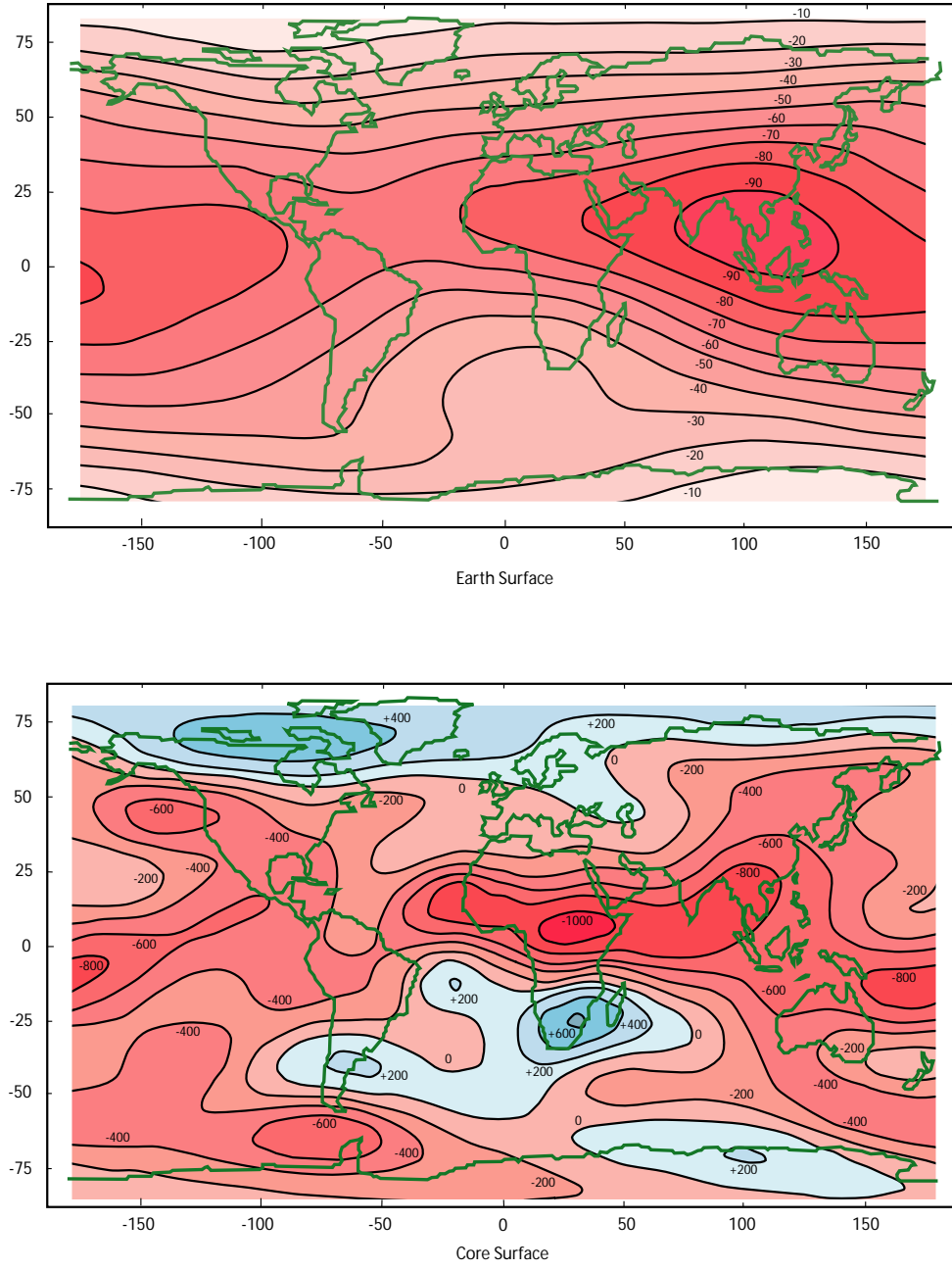


Figure 1. Surface J_{ϕ_1} current density contours for core and Earth surface models. Currents are in Amp/m units.

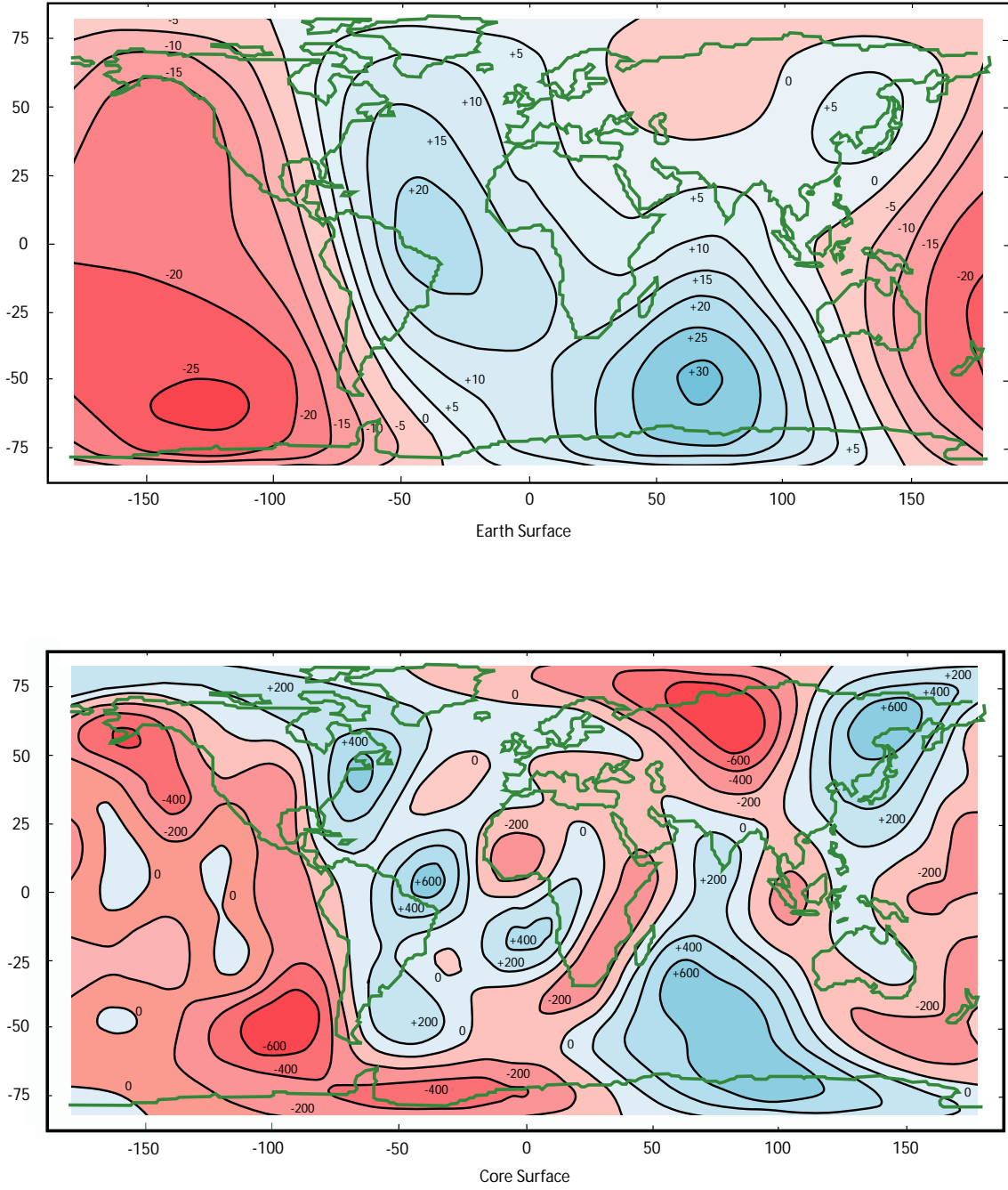


Figure 2. Surface J_{θ_1} current density contours for core and Earth surface models. Currents are in Amp/m units.

In this study, however, it was found that solid sphere (e.g. whole core) current models produced considerably larger errors than current surface models, and the current was

concentrated at the top of the sphere. The (θ_1, ϕ_1) variation of the SVD current solutions J_{θ_1} and J_{ϕ_1} for the core surface and Earth surface models are dissimilar, in that the core surface distributions are considerably more complicated those for the Earth surface models. For example, core surface current profiles for J_{ϕ_1} at longitudes -60° West and 30° East contain two series of alternating negative and positive currents, whereas Earth surface current profiles are positive everywhere. Placing the source structure at the surface of the inner core yields even greater complexity, and the J_{ϕ_1} distribution for this model consists of several alternating belts of negative and positive current. In addition, the prediction error of the core surface model is substantially higher than that for the Earth surface model. Presumably the distance between the current source structure to the MAGSAT data locations is the prime factor controlling these characteristics. The similarity between the Earth surface J_{ϕ_1} current distribution and the X component of the 1980 GSFC(12/83) model at the Earth's surface may also be due to this factor.

The problem of the non-uniqueness of solutions to inverse theory problems has been discussed in some detail in the literature (Backus and Gilbert, 1970; Parker, 1977; Menke, 1989). In the case of the main geomagnetic field, if the source current lies within the core, a poloidal core current structure will produce a toroidal magnetic field which is largely or completely confined to the core, and therefore will not be measurable at the Earth's surface. Hence the currents that actually produce the magnetic field measured at the surface could be minor components of a much larger core current structure. The only limitation on the magnitude of such poloidal currents is due to the ohmic heating constraint. Evidently the surface current models obtained here, which are based on the "natural" (SVD) solution to the geomagnetic inverse problem, are in essence the minimal or simplest current structures that will produce the measured field.

References

- Allredge, L.R. (1980), Circular current loops, magnetic dipoles and spherical harmonic analyses, *J. Geomag. Geoelec.*, 32, 357-364.
- Backus, G. E. and J. F. Gilbert (1970), Uniqueness in the inversion of gross Earth data, *Phil. Trans. R. Soc. London*, A266, 123-192.
- Dongarra, J.J., J.R. Bunch, C.B. Moler, G.W. Stewart (1979), *LINPACK User's Guide*, SIAM, Philadelphia.
- Fraser-Smith, A.C. (1987), Centered and eccentric geomagnetic dipoles and their poles, 1600-1985. *Rev. Geophys.*, 25, 1-16.
- Hansen, P.C., (1990), Truncated SVD solutions to discrete ill-posed problems with ill-determined rank, *SIAM J. Sci. Stat. Comp.*, 11, 503-512.

- Langel, R.A., (1982), The magnetic Earth as seen from MAGSAT, initial results, *Geophys. Res. Lett.*, 9, 239-242.
- Langel, R.A., G. Ousley, J. Berbert, J. Murphy, and M. Settle, (1982), The MAGSAT mission. *Geophys. Res. Lett.*, 9, 243-245.
- Langel, R.A. (1985), The near-Earth magnetic field at 1980 determined by Magsat data, *J. Geophys. Res.*, 90, 2495-2509.
- Langel, R.A., and R.H. Estes (1987), The Main Field, in *Geomagnetism*, edited by J.A. Jacobs, pp. 249-512, Academic Press, London.
- Menke, W. (1989), *Geophysical Data Analysis: Discrete Inverse Theory*, Academic Press, San Diego.
- O'Brien, M.S., and R.L. Parker, (1994), Regularized geomagnetic field modeling using monopoles, *Geophys. J. Int.*, 118, 566-578.
- Parker, R.L. (1979), Understanding inverse theory, *Ann. Rev. Earth Planet. Sci.*, 5, 35-64.
- Peddie, N.W. (1979), Current loop models of the Earth's magnetic field, *J. Geophys. Res.*, 84, 4517-4523.
- Tarantola, A. (1987), *Inverse Problem Theory*, Elsevier, New York.
- Zidarov, D.P., and T.D. Petrova (1979), Presenting the Earth's magnetic field as a field of circular current loops, *C.R. Acad. Bulg. Sci.*, 32, 19-22.